

An Oscillatory Interference Model of Grid Cell Firing

Neil Burgess,^{1,2*} Caswell Barry,^{1–3} and John O'Keefe^{2,3}

ABSTRACT: We expand upon our proposal that the oscillatory interference mechanism proposed for the phase precession effect in place cells underlies the grid-like firing pattern of dorsomedial entorhinal grid cells (O'Keefe and Burgess (2005) *Hippocampus* 15:853–866). The original one-dimensional interference model is generalized to an appropriate two-dimensional mechanism. Specifically, dendritic subunits of layer II medial entorhinal stellate cells provide multiple linear interference patterns along different directions, with their product determining the firing of the cell. Connection of appropriate speed- and direction-dependent inputs onto dendritic subunits could result from an unsupervised learning rule which maximizes postsynaptic firing (e.g. competitive learning). These inputs cause the intrinsic oscillation of subunit membrane potential to increase above theta frequency by an amount proportional to the animal's speed of running in the "preferred" direction. The phase difference between this oscillation and a somatic input at theta-frequency essentially integrates velocity so that the interference of the two oscillations reflects distance traveled in the preferred direction. The overall grid pattern is maintained in environmental location by phase reset of the grid cell by place cells receiving sensory input from the environment, and environmental boundaries in particular. We also outline possible variations on the basic model, including the generation of grid-like firing via the interaction of multiple cells rather than via multiple dendritic subunits. Predictions of the interference model are given for the frequency composition of EEG power spectra and temporal autocorrelograms of grid cell firing as functions of the speed and direction of running and the novelty of the environment. © 2007 Wiley-Liss, Inc.

KEY WORDS: entorhinal cortex; stellate cells; dendrites; hippocampus; place cells; theta rhythm

INTRODUCTION

One of the fundamental questions of systems neuroscience concerns the functional role of temporal characteristics of neuronal firing. One of the most robust examples of temporal coding of a higher cognitive variable is the coding of an animal's current location by the phase of firing of hippocampal pyramidal cells (place cells, O'Keefe and Dostrovsky, 1971) relative to the theta rhythm of the ongoing EEG (O'Keefe and Recce, 1993). Here we examine a computational model which explains this firing pattern as resulting from the interference of two oscillatory contributions to the cell's membrane potential (O'Keefe and Recce, 1993; Lengyel et al.,

2003), and generalize it to explain the strikingly periodic spatial firing pattern of "grid cells" in dorsomedial entorhinal cortex (Hafting et al., 2005).

We briefly review the relevant properties of the firing of place cells and grid cells in their corresponding sections later. First we briefly outline some of the salient aspects of the organization of the hippocampal and entorhinal regions in which they are found. The vast majority of neocortical input to the hippocampus comes via the medial and lateral divisions of the entorhinal cortex (e.g. Amaral and Witter, 1995). However, the connection between entorhinal cortex and hippocampus is by no means unidirectional, with direct connections from hippocampal region CA1 back to the deep layers of entorhinal cortex, and targeting the same dorsoventral level from which it receives connections (from layer III) (Kloosterman et al., 2004). See Witter and Moser (2006) for further details. In addition to place cells and grid cells, cells coding for the animal's current head-direction are found in the nearby dorsal presubiculum (Ranck, 1984; Taube et al., 1990). The theta rhythm is a large amplitude oscillation of 8–12 Hz observed in the EEG of rats as they move around their environment (Vanderwolf, 1969; O'Keefe and Nadel, 1978) which appears to be synchronised throughout the entire hippocampal-entorhinal system (Mitchell and Ranck, 1980; Bullock et al., 1990). Within this system, medial (but not lateral) entorhinal cortex appears to have two distinct properties which will be discussed later: it receives projection from the presubiculum, likely carrying head-direction information, and it contains stellate cells in layer II, which show intrinsic sub-threshold membrane potential oscillations (MPOs) in the theta frequency band (Alonso and Llinas, 1989; Alonso and Klink, 1993; Erchova et al., 2004).

The Dual-Oscillator Interference Model of Place Cell Firing

Hippocampal place cells recorded in freely moving rats fire whenever the animal enters a specific portion of its environment (the "place field," O'Keefe and Dostrovsky, 1971; O'Keefe, 1976). In addition, the cells fire with a characteristic timing relative to the concurrent theta rhythm of the EEG: firing at a late phase on entering the place field and at successively earlier phases as the animal passes through the place field on a linear track (O'Keefe and Recce, 1993). In these situations place cells tend to fire only when the rat is moving in

¹ Institute of Cognitive Neuroscience, University College London, London, United Kingdom; ² Department of Anatomy and Developmental Biology, University College London, London, United Kingdom; ³ Institute of Behavioural Neuroscience, University College London, London, United Kingdom

Grant sponsors: MRC, Wellcome Trust, Biological Sciences Research Council (BBSRC), UK.

*Correspondence to: Neil Burgess, Institute Cognitive Neuroscience, 17 Queen Square, London WC1N 3AR, United Kingdom.

E-mail: n.burgess@ucl.ac.uk

Accepted for publication 1 May 2007

DOI 10.1002/hipo.20327

Published online 27 June 2007 in Wiley InterScience (www.interscience.wiley.com).

one direction along the track (McNaughton et al., 1983). An important feature of this pattern of firing is that the correlation between firing phase and location is better than that between firing phase and time since entering the place field (O'Keefe and Recce, 1993), indicating that it plays a role in encoding location rather than merely being a side-effect of the temporal dynamics of pyramidal cells. In addition, the phase of firing continues to accurately represent location despite large variations in the firing rate (which may encode nonspatial variables such as speed, Huxter et al., 2003).

In open field environments, place cells fire whenever the rat is in the place field irrespective of running direction (Muller et al., 1994). In this situation, firing phase precesses from late to early as the animal runs through the place field irrespective of running direction, such that the cells firing at a late phase tend to have place fields centered ahead of the rat while those firing at an early phase have fields centered behind the rat (Burgess et al., 1994; Skaggs et al., 1996). In this way, firing phase appears to reflect the relative distance traveled through the cells' firing field (or "place field"), see (Huxter et al., 2003).

The phase precession effect can be explained as an interference pattern between two oscillatory inputs, as proposed by O'Keefe and Recce (1993) and elaborated upon by Lengyel et al., (2003). One input, which we refer to as "somatic," has angular frequency w_s , approximately corresponds to the theta rhythm in the extracellular EEG recorded near the soma, and reflects the inputs from the medial septal pacemaker (Petsche et al., 1962; Stewart and Fox, 1990). The second input, which we refer to as "dendritic", has an angular frequency w_d which increases above the somatic frequency with running speed v , that is,

$$w_d = w_s + \beta v, \quad (1)$$

where β is a positive constant.

This latter oscillation is presumed to be an intrinsic oscillation of the dendritic membrane potential, whose frequency increases above theta frequency in response to a speed-dependent input (e.g., from "speed cells," O'Keefe et al., 1998). There is some evidence that dendrites can operate as such a voltage-controlled oscillator (e.g., Kamondi et al., 1998). If the somatic membrane potential sums both inputs, the cell will exceed firing threshold at the peaks of the resulting interference pattern. That is, firing will reflect a "carrier" at the mean frequency of the two oscillations, modulated by an "envelope" at half the difference of the frequencies (the amplitude of the envelope is actually at the difference of the frequencies as it includes the positive and negative lobes). See Figure 1 for details. In the general case of frequencies with unequal amplitudes a_d and a_s , and initial phase difference ϕ_d we have:

$$a_d \cos(w_d t + \phi_d) + a_s \cos(w_s t) = 2a_s \cos((w_d + w_s)t/2 + \phi_d/2) \cos((w_d - w_s)t/2 + \phi_d/2) + (a_d - a_s) \cos(w_d t + \phi_d) \quad (2)$$

Notice that the carrier frequency exceeds theta in a speed-dependent way so that its phase precesses through 180° relative

to theta. Changes in the relative amplitude of the two inputs can result in slight increases or decreases in the amount of phase precession (Lengyel et al., 2003). See Figure 1. Notice also that the spatial scaling factor β determines the length L of each bump in the envelope of the interference pattern:

$$L = 2\pi/\beta. \quad (3)$$

One major discrepancy between this simple model of place cell firing and the experimental data is that most place cells have a single firing field. Thus, one must posit an additional mechanism to account for the absence of out-of-field firing. For example, in the absence of the speed dependent input, the dendritic oscillation may be entrained to theta frequency, but 180° out of phase relative to the somatic input, causing complete destructive interference ($\phi_d = 180^\circ$, see also Lengyel et al., 2003). This would be consistent with the phase reversal seen in theta as the recording location moves from the soma to the apical dendrites (Winson, 1976), suggesting two sources of theta currents in hippocampal pyramidal cells (Brankack et al., 1993; Buzsaki et al., 1986).

Indirect evidence supporting this model was recently reported by Maurer et al., (2005). They compared the intrinsic firing frequencies of place cells recorded from the dorsal hippocampus with those from more ventral locations. They confirmed that the more ventral cells had larger fields (Jung et al., 1994), and related to this there was a corresponding reduction in their intrinsic firing frequency. This intrinsic frequency was defined by the period indicated by the first peak in the temporal autocorrelation of cell firing, and in many interneurons normally occurs at ~ 100 ms, indicating theta-modulation of cell firing. In contrast, the phase precession phenomenon corresponds to an earlier peak in the autocorrelogram of place cells than the typical period of theta in the concurrently recorded EEG (O'Keefe and Recce, 1993). Place cells fire at a slightly higher inter-burst frequency than theta, corresponding to their precession from late to early phases of theta. Maurer et al. (2005) found that the intrinsic frequency of place cell firing was even higher in dorsal hippocampal place cells than more ventral hippocampal place cells. The observed relationship between intrinsic firing frequency and field size indicates that the constant β decreases systematically from dorsal to ventral hippocampus – decreasing the intrinsic frequency of firing and increasing the size of place fields. Or, alternatively, that the somatic frequency w_s decreases from dorsal to ventral and that the dendritic oscillation is multiplicatively related to somatic frequency [i.e., assuming Eq. (1a) below rather than Eq. (1)].

AN INTERFERENCE MODEL OF GRID CELL FIRING

"Grid cells" recorded in the dorsomedial entorhinal cortex of freely moving rats fire whenever the rat enters any one of a set of locations which are distributed throughout the environment at

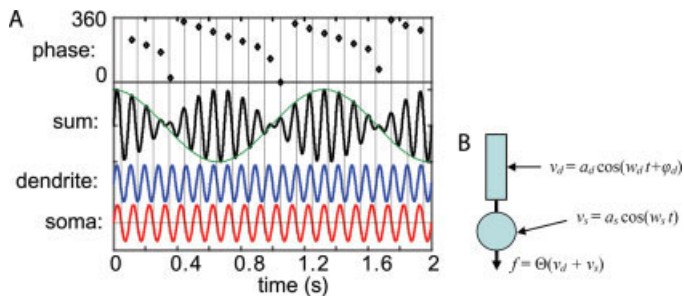


FIGURE 1. A: Dual oscillator interference model of phase precession, showing the sum of an oscillatory somatic input (v_s) at 10 Hz, and an oscillatory dendritic input at 11.5 Hz (v_d). That is, $v_s + v_d$, where $v_s = a_s \cos(w_s t)$, $v_d = a_d \cos(w_d t + \phi_d)$, with $w_s = 10 \times 2\pi$, $w_d = 11.5 \times 2\pi$, $a_s = a_d = 1$, $\phi_d = 0$. The sum of the two oscillations is an interference pattern comprising a high frequency “carrier” oscillation (frequency 10.75 Hz) modulated by a low frequency “envelope” (frequency 0.75 Hz; rectified amplitude varies at 1.5 Hz). B: Schematic showing a cell whose firing rate is the rectified sum of both inputs (Θ is the Heaviside function). The top row of A represents the phase at which peaks of the interference pattern occur—i.e., peaks of the overall membrane potential when summing the dendritic and somatic inputs and thus likely times for the firing of an action potential. [Color figure can be viewed in the online issue, which is available at www.interscience.wiley.com.]

the vertices of an equilateral triangular (or close-packed hexagonal) grid (Hafting et al., 2005). These cells were first reported in layer II, where grid cell firing is independent of the head-direction of the rat. Grid cells have since also been reported to occur in deeper layers of entorhinal cortex, where their firing is often modulated by head-direction (Sargolini et al., 2006). The grids of nearby grid cells have the same spatial scale, but the spatial scale of grids recorded at different recording locations increases with increasing distance from the dorsal boundary of the entorhinal cortex (Hafting et al., 2005). Interestingly, all of the grids within a given animal appear to have the same orientation (Fyhn et al., 2007; Barry et al., 2007). Fyhn et al. (2007) found that, when a rat forages in two different familiar environments, grid cells can show a shift in the overall relationship of the grid to the environment, while place cells remap (i.e., show a random rearrangement of firing rates and locations Bostock et al., 1991). In this situation, the spatial scale of the grid does not change even if the two environments have different sizes (Hafting et al., 2005). However, when grid cells are recorded in a single deformable environment, the grids adjust their spatial scale in response to changes to the size of the environment (Barry et al., 2007), as does place cell firing (O’Keefe and Burgess, 1996).

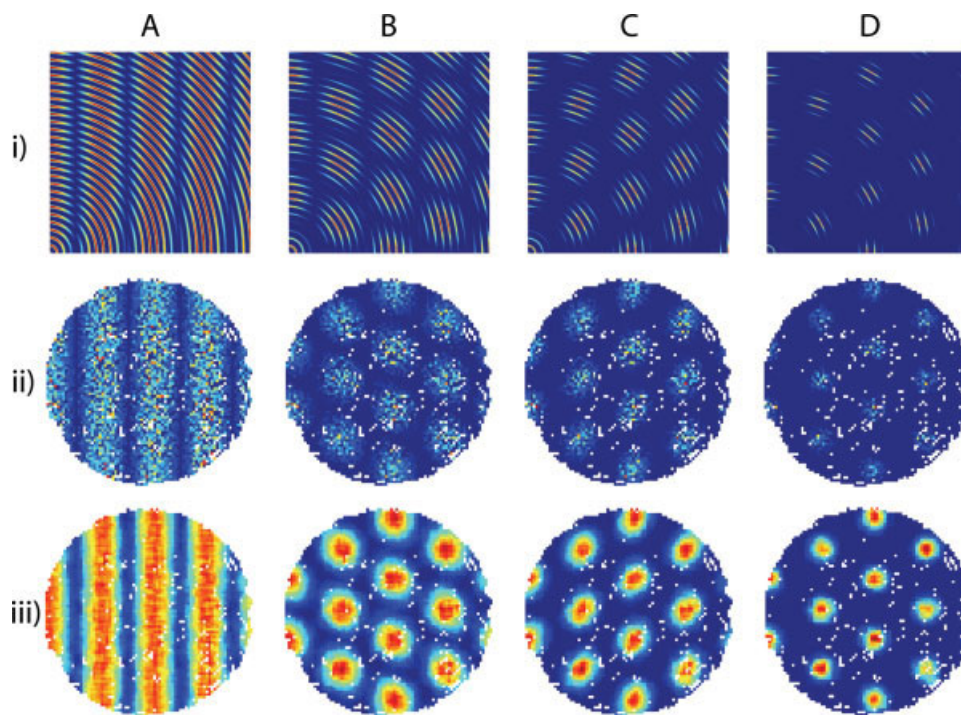


FIGURE 2. Directional interference patterns [see Eq. (5)], showing the positive part of a single directional interference pattern (A, rightward preferred direction), and the product of two (B), three (C) or six (D) such patterns oriented at multiples of 60° to each other. (i) Pattern generated by straight runs at 30 cm/s from the bottom left hand corner to each point in a $78 \times 78 \text{ cm}^2$ box (ii) Pattern generated by averaging the values generated at each location during 10 min of a rat’s actual trajectory while foraging for randomly scattered food in a 78 cm cylinder (white spaces indicate unvisited locations). (iii) As (ii) but shown with 5 cm boxcar smoothing for better comparison with experimental

data. All oscillations are set to be in phase ($\phi_i = 0$) at the initial position (i: bottom left corner; ii: start of actual trajectory—indicated by an arrow in Fig. 5). The plots show $f(\underline{x}(t)) = \Theta(\prod_{i=1}^n \cos(w_i t + \phi_i) + \cos(w_s t))$, for $n = 1$ (A), two (B), three (C) and six (D), with $w_i = w_s + \beta \cos(\theta - \theta_i)$, where s is running speed, θ is missing direction, spatial scaling factor $\beta = 0.05 \times 2\pi \text{ rad/cm}$ (i.e., 0.05 cycles/cm), preferred directions: $\theta_1 = 0^\circ$ (i.e. rightwards), $\theta_2 = 60^\circ$, $\theta_3 = 120^\circ$, $\theta_4 = 180^\circ$, $\theta_5 = 240^\circ$, $\theta_6 = 310^\circ$. Θ is the Heaviside function. All plots are auto-scaled so that red is the maximum value and blue is zero. [Color figure can be viewed in the online issue, which is available at www.interscience.wiley.com.]

O'Keefe and Burgess (2005) noted the intriguing resemblance between the grid-like pattern of firing and the multi-peaked interference pattern (Fig. 1), and that its repeating nature would avoid the need to restrict the speed-dependent input to a single location as required by the place cell model. In addition, we noted the fact that mEC layer II appears to contain a theta generator independent of hippocampal theta, with layer II stellate cells showing subthreshold oscillations of 8–9 Hz (Alonso and Llinas, 1989; Alonso and Klink, 1993; Erchova et al., 2004), and the potential availability in mEC of speed-modulated head-direction information (Sharp, 1996) from the presubiculum (Amaral and Witter, 1995). We then suggested how the above one-dimensional mechanism might be generalized to the two-dimensional grid pattern (Burgess et al., 2005), which will be discussed later. As predicted by the model, layer II grid cells have been subsequently reported to show a similar phase precession effect to that observed in hippocampal place cells (Hafting et al., 2006). In addition, Michael Hasselmo and colleagues were inspired to look for the predicted variation in intrinsic MPOs in layer II stellate cells as a function of their dorsoventral location within medial entorhinal cortex—finding the predicted correspondence to the increase in grid size (Giocomo et al., 2007). They also showed that the frequency of the intrinsic oscillation depends on the time constant of the h-current, which varies dorsoventrally.

2D Interference: Multiple Linear Oscillators

A simple extension of the above linear dual oscillator is to give the dendritic oscillator a “preferred direction” so that phase precesses according to distance traveled along a specific running direction ϕ_d , i.e.,

$$w_d = w_s + \beta s \cos(\phi - \phi_d) \quad (4)$$

The resulting interference pattern when summed with the somatic oscillatory input [i.e., $\cos(w_d t) + \cos(w_s t)$], resembles parallel bands across a 2D environment, perpendicular to direction ϕ_d . As before, the distance from one band to the next is $L = 2\pi/\beta$. See Figure 2A. The phase difference between the dendritic and somatic oscillators effectively integrates speed to give distance traveled along the preferred direction.

The simplest model for hexagonal close-packed grids involves multiplying two or three such interference patterns with preferred directions differing by multiples of 60° , see Figure 2. (Alternatively the patterns could be summed, with the application of a suitable threshold.) Thus we envisage that the interference patterns, produced by each dendritic oscillation interfering with the common somatic input, all multiply at the soma—in the sense that all three resultant oscillations have to be significantly depolarized for the cell to exceed firing threshold overall. For simplicity, we assume that all inputs (one somatic and three dendritic) have amplitude of unity and the cell has a threshold linear transfer function with threshold zero. Thus grid cell firing rate with n dendritic inputs is

$$\begin{aligned} f(t) &= \Theta(\Pi_{i=1}^n (\cos\{[w_s + \beta s \cos(\phi - \phi_i)]t + \varphi_i\} \\ &\quad + \cos\{w_s t\})), \\ &= \Theta(\Pi_{i=1}^n 2\cos\{[w_s + \beta s \cos(\phi - \phi_i)]/2t \\ &\quad + \varphi_i/2\} \cos\{\beta s \cos(\phi - \phi_i)t/2 + \varphi_i/2\}), \quad (5) \end{aligned}$$

where w_s is theta frequency, s is running speed, ϕ is running direction, ϕ_i is the preferred direction, and φ_i the phase offset of the i th dendritic input, β is a positive constant, and Θ is the Heaviside function ($\Theta(x) = x$ if $x > 0$; $\Theta(x) = 0$ otherwise).

Examples of grid cell firing rate as a function of position (“firing rate maps,” i.e. $f(x(t))$), where $x(t)$ is position at time t) are shown in Figure 2, with the number of dendritic inputs $n = 1, 2, 3$, and 6. For preferred directions that vary by multiples of 60° , any combination of two or more linear interference patterns produces hexagonal grids. The exact shape of the firing field at each grid node (i.e., circular or ellipsoidal, and the orientation of the ellipse) for $n = 3, 4$, or 5 depends on the exact choice of preferred directions relative to the direction from the origin (i.e. bottom left corner in Fig. 2i). For example, the plot for $n = 3$ (Fig. 2Ci) has more circular nodes for preferred directions ($0^\circ, 240^\circ, 310^\circ$) than for the ones shown ($0^\circ, 60^\circ, 120^\circ$). Interestingly, the pattern with $n = 6$, comprised of linear interference patterns in all six directions separated by multiples of 60° , has nodes which are roughly circular for all directions. Anatomically, the layer II stellate cells have 4–8 (mode 5) noticeably thick proximal dendrites (Klink and Alonso, 1997a), possibly reflecting the likely range of numbers of subunits.

The symmetrical model with $n = 6$ subunits (or $n = 4$ with 2 pairs of opposing preferred directions) is interesting for a second reason: unlike its component subunits, the cell would not show phase precession. Each subunit contains a linear interference pattern with a carrier at a frequency above theta when the rat is running along its preferred direction, resulting in phase precession when summed with the somatic theta input. (We note two important caveats. First, in this basic model the carrier would have a frequency below theta when the rat ran in the opposite direction—producing reverse phase precession, see Variants of the basic model, later. Second, phase precession would also require a mechanism for setting the initial phase on entry to each firing field, as in the place cell model, earlier). However, each interference pattern is multiplied by one with the opposite preferred direction. Significant firing will only occur when both interference patterns have similar phase, i.e., at the centre of the field. We note that, unlike layer II grid cells which show phase precession, grid cells in layer III fire phase-locked to theta (Hafting et al., 2006).

Figure 2 also illustrates the dependence of the firing rate at a particular location on the trajectory by which the rat has reached that location (and the initial phases of all the oscillators at the start of the trajectory). Although the envelopes of the linear interference patterns remain fixed in space irrespective of trajectory, the value of the carrier waves, and therefore their product, will depend on the precise trajectory taken to reach a given location from an initial phase configuration (or reset point, see Fig. 5 later). The plots in Figure 2A show the firing rate at each loca-

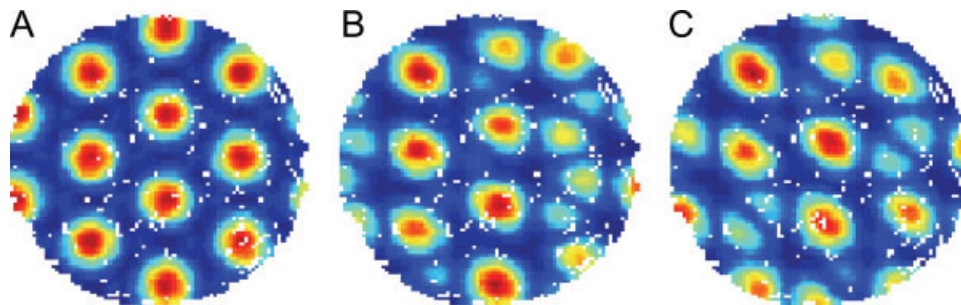


FIGURE 3. Simulation of “grid cell” firing as the product of three linear interference patterns with different combinations of preferred directions [see Eq. (5)]. Simulated cells with regular grid firing patterns achieve high firing rates more often than those with irregular patterns, so long as collinear preferred directions excluded. (A) The most frequently high-firing grid cell (firing at 90% of maximum firing rate, 8 Hz, 1,310 times in the 28,125 locations sampled by a rat in 10 min, same trajectory as Fig. 2). (B) The median frequency high-firing cell is shown in the middle

(433 times). (C) The least often high-firing cell on the right (228 times). Cell firing rate was simulated as the product of the firing envelopes of the three inputs to each cell, to facilitate speed and reliability. All unique combinations of preferred directions ($\theta_1, \theta_2, \theta_3$) selected from ($0^\circ, 10^\circ, \dots, 350^\circ$) such that all angles differ by at least 20° were simulated. These firing rate maps are shown with 5 cm boxcar smoothing for better comparison with experimental data. [Color figure can be viewed in the online issue, which is available at www.interscience.wiley.com.]

tion for straight runs of constant speed to that location from the origin (where all dendritic oscillators are initially in phase with theta). The frequency of the carrier wave for a linear interference pattern is the mean of the theta frequency somatic input and the dendritic frequency (which varies around theta frequency according to running direction and speed). For runs of constant velocity (upper plots) the dendritic frequency is constant, so the phase of the carrier can be seen varying simply with the duration of the run to a given location (note concentric rings), and is slightly higher when running in the preferred direction than in the orthogonal direction (e.g., rightwards vs. upwards in Fig. 2A). For more complicated trajectories (Fig. 2B), the relative phases of the carrier waves for each linear interference pattern, and so the firing rate at any given moment, are much less predictable. This may help to explain the unusually high variance in place cell firing (and of grid cell firing, we would predict) over different runs (Fenton and Muller, 1998).

Indirect evidence for the presence of at least three linear interference patterns (as opposed to only two) is that self-organization of three inputs to a cell would more likely produce regular hexagonal close-packing. If three dendritic interference patterns are chosen with random directions, the frequency with which all three are simultaneously strongly active (i.e. their product is near its maximum) will be greatest if the three patterns are collinear, or else when they differ by multiples of 60° from each other, see Figure 3. The same argument holds for additional patterns being oriented at further multiples of 60° . Thus self-organizing learning rules in which plasticity is triggered by maximal or near-maximal levels of post-synaptic activity are likely to converge on a regular hexagonal grid, so long as collinear inputs are excluded. In addition, we note that the connection of appropriate subsets of head-direction cells onto grid cells is likely determined during a large-scale developmental process, given that all of the grids within an animal appear to have the same orientation (Fyhn et al., 2007; Barry et al., 2007).

Figure 4 shows a schematic of a grid cell driven by three linear interference patterns from three subunits driven by inputs with

preferred directions differing by multiples of 60° from each other. The rat is shown running perpendicular to the preferred direction of one of the subunits (blue), so the MPO for this subunit oscillates at theta frequency. However, it is running close to the preferred directions of the other two subunits which therefore oscillate at above theta frequency (red and green, rat shown running at around 30° from their preferred directions). Spikes would be fired at the peaks of the product of the three interference patterns generated by these dendritic MPOs interacting with somatic theta.

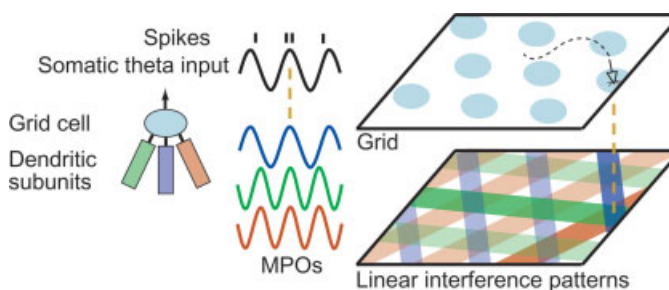


FIGURE 4. Schematic of the interference model of grid cell firing. Left: Grid cell (pale blue) receiving input from three dendritic subunits (red, blue, green). Middle: Spikes, somatic theta input (black) and dendritic membrane potential oscillations (MPOs, red, blue, green). The rat is shown (upper right) running perpendicular to the preferred direction of one of the subunits (blue), so the MPO of this subunit oscillates at theta frequency. Since the rat is running approximately along the preferred directions of the other two subunits (red and green, i.e. within 30° of their preferred directions), these MPOs oscillate above theta frequency. Spikes are shown at the times of the peaks of the product of the three interference patterns each MPO makes with the somatic theta input. The locations of the peaks of the envelopes of the three interference patterns are shown on the environment in the corresponding colors (red, green and blue stripes, lower right). The locations of grid cell firing are shown in pale blue and occur in the environment wherever the three envelopes all peak together (upper right). [Color figure can be viewed in the online issue, which is available at www.interscience.wiley.com.]

terference patterns from each dendrite are shown on the environment in the corresponding colors (red, green, and blue stripes, lower right). The locations of grid cell firing are shown in pale blue and occur in the environment wherever these envelopes intersect (upper right).

Phase Resetting, Correction of Cumulative Error, and Interactions With Hippocampus

One consideration when multiplying three (or more) linear interference patterns is that they have to have the correct relative phases to align, that is, there is one (or more) degree of freedom to be set (e.g., the phase of the third dendritic oscillator so that it aligns with the grid formed by the first two). In addition, the phases of the dendritic oscillations determine the grid location in space. So far we have assumed perfect knowledge of running speed and direction; however, this is subject to error (e.g., Etienne et al., 1996), with a cumulative effect on the grid's location in space. The fact that grids are reliably located from trial to trial implies that they rapidly become associated to environmental landmarks within a familiar environment. This can be done by resetting all dendritic oscillators to the same phase as the somatic (theta) input at the location of a grid node. We propose that input from place cells serves this function, see later. There is no direct evidence that this occurs, although phase resetting of the theta rhythm by sensory stimuli has been observed (e.g., Buzsáki et al., 1979; Williams and Givens, 2003).

As pointed out in (O'Keefe and Burgess, 2005), the association to environmental information is likely mediated by place cells, as their unimodal firing fields would be easier to associate to the sensory information specific to a given environmental location. Thus, on initial exposure to an environment, place cells whose firing peaks coincide with the peak of a grid node, would form connections to the grid cell to maintain the environmental location of the grid node during exposure to the now familiar environment. To implement the phase-reset mechanism, these connections would enable the place cells' peak firing to reset the grid cell's dendritic oscillations to be in phase with the somatic (theta) input. This would be the natural phase for such a reset, given that place cells' peak firing rate also occurs in phase with theta (a consequence of the hippocampal phase precession effect), and the coordination of theta throughout the hippocampal-entorhinal system (Mitchell and Ranck, 1980; Bullock et al., 1990). See Figures 5 and 6.

The model also sees the grid cells as providing the path integrative input to place cells, which will occur if the grids which overlap at the location of the place field provide input to the place cell, while the place cells provide the environmental sensory input to maintain a stable position of the grids in the environment (see O'Keefe and Burgess, 2005). This would be consistent with the known anatomy, whereby projections from medial entorhinal cortex project to similar regions of CA1 from which they receive return projections (Kloosterman et al., 2004). The environmental sensory input to place cell firing includes local olfactory, tactile, visual, and possibly auditory information most likely transmitted via lateral entorhinal cortex. Sensory informa-

tion concerning the locations of physical boundaries to motion may play an especially important role here, see discussion of the relationship to "boundary vector cell" inputs to place cells below.

In our original description of this model (Burgess et al., 2005), we investigated the possibility of phase reset at a single environmental location, which suffices to prevent significant accumulation of error, see Figure 6. Local groups of grid cells all have similar grids but with different spatial phases (Hafting et al., 2005), in our model, these correspond to different values of the phase difference between dendritic and somatic oscillations at any given location (i.e., ϕ_1 , ϕ_2 , and ϕ_3). In each local group, the grid cell whose firing usually peaks at the reset location would be the one to be phase-reset via learned association from place cells with peak firing at that location. The phase of firing of the reset grid cell would then have to propagate to the other members of the local group (with different phases) via local recurrent circuitry with appropriate directional and temporal properties. That is, grid cells which fire just after the reset cell, given the current running direction, receive inputs from it with a small but speed-dependent transmission delay. This proposed function for the local circuitry has similar requirements to the commonly proposed function of shifting of a bump of activity along a continuous attractor (Fuhs and Touretzky, 2006; McNaughton et al., 2006).

In favor of a single reset location, Hafting et al. (2005) presented evidence that the firing pattern of grid cells did not change its spatial scale between recordings in a large cylinder and a small cylinder. Phase resetting at a single location would not change grid scale in this situation, even though the location and shape of place fields is consistently distorted by such manipulations within a familiar environment (O'Keefe and Burgess, 1996; Barry et al., 2006). This would also correspond to Redish and Touretzky's (1997) idea of the hippocampus providing a single re-set to an entorhinal path-integrator. In addition, some locations do seem to be more salient than others, for example the start and ends of a linear track. In some circumstances of practiced running on a linear track, the theta rhythm appears to be phase reset at the start of each run (unpublished observation), see further discussion later.

However, we now find that changing the shape and size of a familiar environment does distort the grid-like firing patterns in a similar way to those of place cells, changing their spatial scale in the same direction as the change to the environment but by a lesser amount (around 50%, Barry et al., 2007). This would be consistent with a simpler model in which a grid cell can be reset at the locations of several of its grid nodes via learned associations from place cells with firing peaked at the centre of the grid node in question. It is possible that boundaries to physical motion provide particularly salient information for triggering phase-resetting, see Discussion later.

Variants of the Basic Model

We note that the frequencies of the dendritic and somatic oscillations could have a multiplicative rather than additive relationship i.e., Eq. (1) could become:

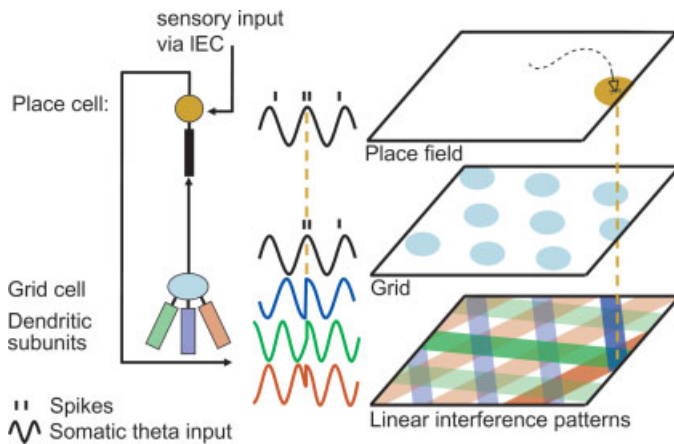


FIGURE 5. Schematic of the association of grid to environment via phase reset of grid cells by place cells. **Left:** Diagram showing anatomical connection from mEC grid cell (pale blue) with three dendrite subunits (green, blue, red) to hippocampal place cell (gold) and feedback from place cell onto the dendrites of the grid cell. **Center:** the maximal firing of the place cell occurs in phase with theta (above, dashed line), and resets dendritic membrane potentials to be in phase with theta (below), **Right:** the path of the rat in the open field and the place cell's firing field (gold, above). In a familiar environment connections from the place cell to the grid cell are developed due to their coincident firing fields (right: above and middle). These connections enable maximal firing of the place cell to reset the phases of the grid cell's dendritic membrane potential oscillations (MPOs) to be in phase with theta—forcing the grid to stay locked to the place field at that location, by ensuring that the envelopes of the three dendritic linear interference patterns coincide at the location of the place field (below right). Sensory input from the environment (especially boundaries), via lateral entorhinal cortex (IEC), keeps the place field locked to the environment. For convenience, only one place cell and one grid cell are shown—in practice we would expect multiple grid cells (with firing at the place field) to project to the place cell, and multiple place cells (with coincident place fields) to project to the grid cell. See Figure 4 for details of the grid cell model. [Color figure can be viewed in the online issue, which is available at www.interscience.wiley.com.]

$$w_d = w_s(1 + \beta s), \quad (1a)$$

and Eq. (4) could become:

$$w_d = w_s(1 + \beta s \cos(\phi - \phi_d)). \quad (4a)$$

In this case, the spatial scale L of hippocampal place fields or entorhinal grids becomes:

$$L = 2\pi/(\beta w_s) \quad (3a)$$

For grids, L gives the spacing for each linear interference pattern, the nodes are separated by $\sqrt{3} L/2$, (see also, Giacomo et al., 2007). However, if w_s relates to the theta rhythm and this is constant throughout the hippocampal-entorhinal system (Mitchell and Ranck, 1980; Bullock et al., 1990), the two variants of the model are indistinguishable unless global variations in theta frequency occur (see later). Giacomo et al. (2007) argue that the dorsoventrally decreasing intrinsic oscillatory frequencies they found in medial entorhinal layer II in vitro reflect a variation in w_s in Eq. (4a) corresponding to a dorsoventral increase in grid size given by Eq. (3a). This is reasonable since the recordings were made in the soma. However, their results could indicate a dorsoventral reduction of β : reducing the dendritic oscillation frequency w_d [in Eqs. (4) or (4a)] and increasing grid size via Eqs. (3) or (3a).

One aspect of the model deserves further scrutiny. The linear interference patterns, whose product generates grid cell firing, result from modulation of the difference between dendritic and somatic oscillators by the cosine of running direction. Each linear pattern shows the familiar phase precession relative to theta (assumed to reflect the somatic oscillator, i.e. from late phase to earlier phases) as the rat runs in the “preferred direction.” However, it shows the reverse pattern when the rat runs in the opposite direction—something not seen in place cell firing, in which precession is always late-to-early, even in the open field (Burgess

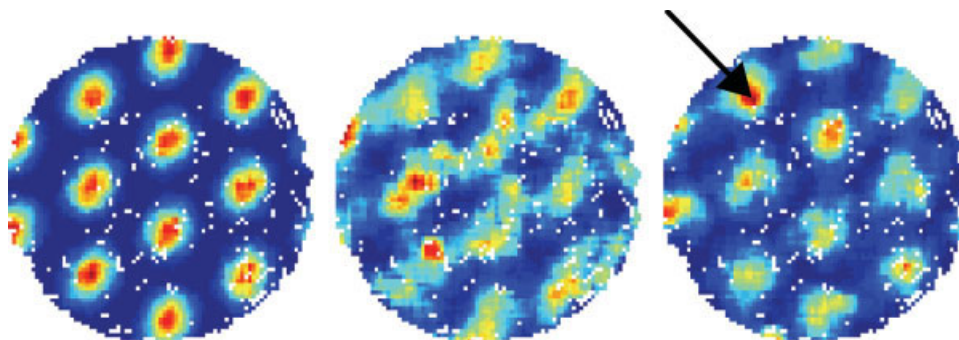


FIGURE 6. Effect of error in speed s and heading θ on simulated grid cell firing, and correction by phase resetting (same trajectory and simulated grid cell as Fig. 2C). **Left:** No error. **Middle:** Error in the estimate of current direction (addition of random variable from Normal distribution $N(0, 10^\circ)$) and distance traveled (multiplication by $1 + \delta$, where δ is drawn from $N(0, 0.1)$) for each time step ($1/48s$). **Right:** Similar error to B, but with phases reset

to $\phi_1 = \phi_2 = \phi_3 = 0$ whenever the animal visits a single location within the 78 cm cylinder (i.e. within 2 cm of the arrow: reset 84 times in 10 min). These firing rate maps are shown with 5 cm boxcar smoothing for better comparison with experimental data. [Color figure can be viewed in the online issue, which is available at www.interscience.wiley.com.]

et al., 1994; Skaggs et al., 1996) where place cells fire for all running directions. When the rat runs perpendicular to the preferred direction, there is no phase precession in the dendritic subunit in question (the dendrite has the same frequency as the soma), although there will be precession in subunits with different preferred directions.

An alternative model for each linear interference pattern could produce late-to-early phase precession in both preferred and opposite directions (and zero precession in perpendicular directions). In this model, rather than one oscillator at theta frequency and one varying in frequency according to running speed and direction (the “somatic” and “dendritic” oscillators respectively earlier), two dendritic oscillators each increase from theta frequency in response to movement in their two opposing preferred directions, and otherwise remain at theta frequency. That is,

$$\begin{aligned}w_{d1} &= w_0 + \beta s \Theta\{\cos(\phi - \phi_{d1})\}; \\w_{d2} &= w_0 + \beta s \Theta\{\cos[\phi - (\phi_{d1} + \pi)]\}.\end{aligned}\quad (6)$$

In this case the most common frequency for any subcomponent is w_0 , which presumably corresponds to the extracellular theta rhythm, while cell firing occurs at higher frequency due to the influence of any subcomponents with preferred directions within 90° of the animal’s direction of motion. Thus theta phase precession will always occur with the same sense: from late to early. This model is similar to the basic model above with $n = 6$ but adds pairs of dendritic oscillators with opposing preferred directions before multiplying the three resulting interference patterns together, and does not require the frequencies of dendritic oscillations to fall below theta.

Finally, we have proposed that multiple oscillators reside in different dendritic subunits, each producing a linear interference pattern. However, a possible alternative is that each linear interference pattern arises in a single grid cell (i.e. the interference between a single voltage-controlled MPO and a theta frequency input), and that the multiplicative interaction of several linear interference patterns arises as a network property of several locally connected grid cells. This would predict that disrupting the action or formation of the necessary local connections should reduce the observed grid-like firing patterns to linear interference patterns.

DISCUSSION

We have outlined a two-dimensional generalization of the one-dimensional interference model of hippocampal theta phase precession (O’Keefe and Recce, 1993; Lengyel et al., 2003) to account for the properties of the firing of grid cells in entorhinal cortex (Hafting et al., 2005)—following our own suggestion of a link between these two phenomena (O’Keefe and Burgess, 2005). The phase of the MPO in each dendritic subunit relative to somatic theta (in the basic model, or relative to the other oscillation in the alternative paired oscillation model) effectively integrates speed in a preferred direction to give distance traveled

in that direction. The presence of two or more subunits with different preferred directions allows the overall grid to perform path integration in two-dimensions. Below we discuss some of the predictions arising from this model.

Experimental Predictions for Intrinsic Frequencies in Cell Firing and EEG

The oscillatory interference model of place cell firing (O’Keefe and Recce, 1993; Lengyel et al., 2003) makes specific predictions for intrinsic firing frequencies, as judged by the autocorrelogram, and for the theta rhythm of the EEG. If the theta rhythm of the EEG corresponds to w_s , place cells should have a slightly higher intrinsic firing frequency $(w_d + w_s)/2$ corresponding to the carrier frequency in Eq. (2). This was shown to be the case by O’Keefe and Recce (1993). A subset of hippocampal interneurons or “theta cells,” which are presumed to play a role in setting the frequency of the theta rhythm, (e.g., Somogyi and Klausberger, 2005), should show an intrinsic frequency similar to theta (w_s). In addition, the difference between intrinsic firing frequency and theta frequency is $(w_d - w_s)/2 = \beta s/2$ and so should increase with running speed s and decrease with field size L (since $L = 2\pi/\beta$). A decreased intrinsic firing frequency coupled to an increase in place field size between dorsal and more ventral locations in the hippocampus was found for place cells (but not theta cells) by Maurer et al. (2005). This indicates a systematic reduction in the intrinsic oscillatory response of the dendrite to its speed-related input (i.e., a reduction in β) dorsoventrally, bringing it closer to the theta frequency which is constant throughout the hippocampus (Bullock et al., 1990).

If grid cell firing is also driven by oscillatory interference, these predictions should also hold for grid cells, which we investigate later. One further prediction is made by an alternative model of grid cell firing (Blair et al., 2007), which posits interference between theta cells whose firing follows a micro hexagonal grid pattern at theta scale. That is, in an animal running at constant speed, the firing pattern would describe a close-packed hexagonal grid across the environment with the distance between neighboring peaks equal to the distance moved in one theta cycle. If pairs of such cells have micro grids of slightly different scale or orientation, and this difference increases with running speed, then their interference pattern will be a microgrid at theta scale (the carrier) modulated by a large-scale hexagonal grid (the envelope). Although no mechanism is described for the generation of the microgrids, the model provides an elegant 2D generalization of the 1D dual oscillator model, assuming that pairs of such microgrid theta cells drive the firing of grid cells. Interestingly, it predicts a modulation of intrinsic frequency by movement direction. Thus, when running along the 6 principal direction of the grid, the grid cell’s intrinsic firing frequency should be approximately equal to theta frequency, but should be slower by a factor $\sqrt{3}$ when running in the intervening directions.

An interesting observation on grid cell firing is the apparent increase in spatial scale when rats are exposed to an environment sufficiently novel to cause global remapping of place cells (Fyhn et al., 2006). Such a nonspecific effect might be mediated by a

global change in theta frequency with novelty. As we noted previously (O'Keefe and Burgess, 2005) there appear to be two thetas with different frequencies present in the hippocampus and mEC: the movement related cholinergically-independent theta with frequency 8–9 Hz and a lower frequency atropine-sensitive frequency of around 6 Hz (Kramis et al., 1975; Klink and Alonso, 1997b). In the basic additive model (Eq. 4), an increase in theta frequency would result in increased grid scale [via Eq. (3)]. However, the alternative multiplicative model [Eq. (4a)] would predict that decreased theta frequency would result in increased grid scale [via Eq. (3a)]. Thus, if novelty related grid expansion does reflect a change in theta frequency, we would be able to distinguish between the two variants of the model by whether theta frequency increases or decreases. A decrease in overall theta frequency in the new environment would be most consistent with cholinergic signaling of environmental novelty in the hippocampal formation (e.g., Thiel et al., 1998; Giovannini et al., 2001; for reviews see: Carlton, 1968; Gray and McNaughton, 1983; Hasselmo, 2006), and would indicate the multiplicative model.

Potential to Explain Other Aspects of Grid Cell Firing

One aspect of the grid cell firing which we have overlooked so far is that the grid pattern is not always perfectly symmetrical. Thus, several of the examples in Hafting et al. (2005) show bandiness—as if the linear interference pattern in one direction is dominating those in the other two directions. This might result from one dendritic subunit having a stronger input to the cell body than the others, or there being more than three subunits, so that some directions become over-represented. This latter situation would be consistent with the operation of unsupervised learning of inputs onto dendrites which maximizes cell firing (for which inputs must be aligned or differ by multiples of 60°).

Other irregularities in the grids might be caused by inputs onto the dendrites whose preferred directions do not differ by exact multiples of 60°. Even directions differing by as little as 20° produces grid-like patterns with strong modulations (see Fig. 3). In addition, modulations of firing rate across the nodes of a regular grid could be caused by the association of place cells to grid cells (see also Fuhs and Touretzky, 2006). We have argued that association to environmental stimuli is required by the spatial stability of the grids over time, and that place cells provide the appropriate representation to mediate such an association, based on the co-occurrence of firing in grid cells and place cells whose firing field overlaps with one of the grid nodes (O'Keefe and Burgess, 2005). Of course, once these associations have been formed, movement of place fields, for example in response to manipulations of environmental size (Muller and Kubie, 1987; O'Keefe and Burgess, 1996), would cause some deformation of the grid. Grids do not change in size when the animal is moved between two different familiar boxes of different size (Hafting et al., 2005). However, recent evidence indicates that grids are spatially deformed when a single familiar environment is

changed in shape or size, although by only 50% of the environmental change (Barry et al., 2007).

Finally, we note that the firing of grid cells in deeper layers of mEC than layer II (presumably pyramidal cells rather than stellate cells) can be modulated by the animal's direction of running (Sargolini et al., 2006). Since the cells (in layer III at least) do not show phase precession (Fyhn et al., 2006), it is not clear what their relationship is to our model, or whether their grid-like firing pattern is generated in layer II. However, the approximately rectified cosine tuning of these directional grid cells is certainly reminiscent of the directional modulation of Eq. (6).

Relationship to “Boundary Vector Cell” Inputs to Place Cells, Environmental Deformations, and Slow Remapping

Changes in place fields induced by geometric manipulation of a familiar enclosure are consistent with the boundary vector cell (BVC) model of place cell firing. The model explains firing as the thresholded sum of inputs tuned to detect the presence of boundaries at specific distances and allocentric directions (O'Keefe and Burgess, 1996; Hartley et al., 2000; Barry et al., 2006). BVC-like firing patterns have been seen in subicular cells (Sharp, 1999; Barry et al., 2006). In the present model, these BVCs, along with local cues, would simply form a major part of the sensory input to place cells via lateral entorhinal cortex.

However, there is also a path integrative component to BVCs. For instance, expanding the environment along one-dimension can reveal the separate contributions of two BVCs responding at specific distances from the two boundaries in that dimension. In this situation, each BVC has a higher firing rate when the rat is heading away from the corresponding boundary than when it is heading towards it; implying that integration of the recent path from the boundary contributes to the BVC response (Gothard et al., 1996; O'Keefe and Burgess, 1996). The input from medial entorhinal grid cells to place cells can be seen as providing this (path integrative) component of the BVC input to place cells. Grid cells which are phase-reset by place cells driven by sensory input (be it visual, tactile, or even auditory) from a boundary in a particular direction will maintain their grid in position relative to that boundary following deformation of the environment. The subsets of these grid cells projecting to a given place cell will thus provide the path-integrative component of a BVC tuned to the boundary in that direction. One role of the direction-dependent grid cells found in deeper layers of entorhinal cortex (Sargolini et al., 2006) might be to be reset by the boundary to motion in the preferred direction, and thus mediate the effect of place cell inputs to deeper layers back up to layer II. The additional strength of sensory input to place cells at the environmental boundary makes these likely reset locations and would be consistent with the higher firing rates and narrower place fields often found there (Muller et al., 1987). Overall, the hippocampal-entorhinal system would thus represent location taking into account both sensory and path-integrative information mediated by lateral and medial entorhinal cortices, respectively (see also Redish and Touretzky, 1997).

Further simulation will be required to see whether this model accounts for four further observations: (1) That when place fields stretch when a linear track is extended in length, the rate of phase precession adjusts to match the field length (Huxter et al., 2003); (2) That a slow return of grids to their intrinsic scale over the course of repeated environmental deformations (i.e. they slowly become insensitive to the deformation, Barry et al., 2007) may drive the slow remapping of place cells between the different arena shapes in this situation (Lever et al., 2002) so that sensory inputs and grid cell inputs to place cells can become realigned in the different shapes; (3) That grids can also squash and stretch in response to environmental deformation (Barry et al., 2007), possibly resulting from phase-resetting by boundaries in all direction, or from associations between grid cells reset by boundaries in different directions (these associations may be mediated by place cells, O'Keefe and Burgess, 2005); (4) The observation that each turn in a maze of multiple hairpin turns resets the spatial phase of the grid for the subsequent run (Derdikman et al., 2006).

CONCLUSION

The model described here builds upon previous dual oscillator interference models of the phase of firing of hippocampal place cells relative to the EEG theta rhythm (O'Keefe and Recce, 1993; Lengyel et al., 2003). It provides a "path integration" mechanism for integrating neural firing reflecting running speed and direction to produce a periodic representation of position: the firing of grid cells (Hafting et al., 2005). The firing of grid cells likely drives the firing patterns of hippocampal place cells, providing a more unimodal representation of position more suitable for association to sensory input from the environment, or for use in memory for spatial location (Fuhs and Touretzky, 2006; McNaughton et al., 2006; O'Keefe and Burgess, 2005). In addition, we have described a phase-reset mechanism by which the inevitable cumulative error in integration can be corrected by place cells receiving environmental sensory input so that the grid cell firing pattern maintains a fixed relationship to the environment.

In brief, the model proposes that the firing of neurons resembling speed-modulated head-direction cells is integrated in the phase of the MPOs in dendritic subunits of layer II stellate cells in medial entorhinal cortex: producing a periodic representation of distance traveled in that direction. Integration occurs via an oscillatory interference mechanism in which the speed \times direction signal serves to increase the frequency of an intrinsic MPO in the dendritic subunit above the frequency of a theta-related input to the cell body. As the rat moves around its environment, the envelope of the resulting interference pattern forms a plain wave across the environment (see Fig. 2). At the cell body, the interaction of the currents from multiple dendritic subunits, each receiving input with a different directional tuning, will form a two-dimensional interference pattern across the environment (see Fig. 2). The resulting pattern of firing will resemble that of a grid cell, with a perfect hexagonal close-packed pattern

resulting from directions differing by multiples of 60° (see Fig. 3). Learned associations to place cells with place fields overlapping a given node of the grid serve to adjust the phase of the grid cell's dendritic subunits so that the grid-node maintains a constant position in space (see Figs. 5 and 6).

Our model provides an alternative to models of grid cells in which path integration occurs by shifting a bump of activity around within a continuous attractor representation supported by recurrent connections (Fuhs and Touretzky, 2006; McNaughton et al., 2006). Although the effects of recurrent connections among grid cells might be added to our model to maintain the relative locations of the grids and enhance their stability and precision, we have focussed on the oscillatory properties of the layer II stellate cells as the basic mechanism for the formation of grid cell firing. One advantage of this emphasis is that we can make contact with, and predictions for, the physiological properties of these cells and their interaction with the theta rhythm. In addition it suggests that medial entorhinal cortex is uniquely adapted to perform path integration due to the presence of both intrinsic subthreshold oscillations and input from the head-direction system via presubiculum in medial but not lateral entorhinal cortex (Alonso and Klink, 1993; Amaral and Witter, 1995; Tahvildari and Alonso, 2005), see also (Witter and Moser, 2006). More generally, we hope to begin to explore the mechanisms surrounding the oscillatory interactions between entorhinal cortex and hippocampus during memory formation in humans (e.g., Fell et al., 2003).

Acknowledgments

This model was previously presented as a poster at the Computational Cognitive Neuroscience Conference, Washington DC, 2005: N. Burgess, C. Barry, K.J. Jeffery, J. O'Keefe: "A Grid and Place cell model of path integration utilizing phase precession versus theta." Authors acknowledge useful discussions with Michael Hasselmo, Tad Blair, Peter Dayan, and Kathryn Jeffery.

REFERENCES

- Alonso A, Klink R. 1993. Differential electroresponsiveness of stellate and pyramidal-like cells of medial entorhinal cortex layer II. *J Neurophysiol* 70:128–143.
- Alonso A, Llinas RR. 1989. Subthreshold Na^+ -dependent theta-like rhythmicity in stellate cells of entorhinal cortex layer II. *Nature* 342:175–177.
- Amaral DG, Witter MP. 1995. The hippocampus. In: Paxinos G, editor. *The Rat Nervous System*, 2nd ed. New York: Academic Press. pp 443–493.
- Barry C, Hayman R, Burgess N, Jeffery KJ. 2007. Experience-dependent rescaling of entorhinal grids. *Nature Neurosci* 10:682–684.
- Barry C, Lever C, Hayman R, Hartley T, Burton S, O'Keefe J, Jeffery K, Burgess N. 2006. The boundary vector cell model of place cell firing and spatial memory. *Rev Neurosci* 17:71–97.
- Blair HT, Welday AC, Zhang K. 2007. Scale-invariant memory representations emerge from moiré interference between grid fields that produce theta oscillations: A computational model. *J Neurosci* 27:3211–3229.

- Bostock E, Muller RU, Kubie JL. 1991. Experience-dependent modifications of hippocampal place cell firing. *Hippocampus* 1:193–205.
- Brankack J, Stewart M, Fox SE. 1993. Current source density analysis of the hippocampal theta rhythm: Associated sustained potentials and candidate synaptic generators. *Brain Res* 615:310–327.
- Bullock TH, Buzsaki G, McClune MC. 1990. Coherence of compound field potentials reveals discontinuities in the CA1-subiculum of the hippocampus in freely-moving rats. *Neuroscience* 38:609–619.
- Burgess N, Recce M, O'Keefe J. 1994. A model of hippocampal function. *Neural Networks* 7:1065–1081.
- Burgess N, Barry C, Jeffery KJ, O'Keefe J. 2005. A grid and place cell model of path integration utilizing phase precession versus theta. Unpublished Poster—Computational Cognitive Neuroscience Conference, Washington, DC.
- Buzsaki G, Grastyan E, Tveritskaya IN, Czopf J. 1979. Hippocampal evoked potentials and EEG changes during classical conditioning in the rat. *Electroencephalogr Clin Neurophysiol* 47:64–74.
- Buzsaki G, Czopf J, Kondakor I, Kellenyi L. 1986. Laminar distribution of hippocampal rhythmic slow activity (RSA) in the behaving rat: Current-source density analysis, effects of urethane and atropine. *Brain Res* 365:125–137.
- Carlton PL. 1968. Brain acetylcholine and habituation. *Prog Brain Res* 28:48–60.
- Derdikman D, Fyhn M, Hafting T, Moser MB, Moser EI. 2006. Breaking up the entorhinal grid in a hairpin maze. *Soc Neurosci Abstr* 68.10.
- Erchova I, Kreck G, Heinemann U, Herz AV. 2004. Dynamics of rat entorhinal cortex layer II and III cells: Characteristics of membrane potential resonance at rest predict oscillation properties near threshold. *J Physiol* 560:89–110.
- Etienne AS, Maurer R, Seguinot V. 1996. Path integration in mammals and its interaction with visual landmarks. *J Exp Biol* 199:201–209.
- Fell J, Klaver P, Elfadil H, Schaller C, Elger CE, Fernandez G. 2003. Rhinal-hippocampal theta coherence during declarative memory formation: Interaction with gamma synchronization? *Eur J Neurosci* 17:1082–1088.
- Fenton AA, Muller RU. 1998. Place cell discharge is extremely variable during individual passes of the rat through the firing field. *Proc Natl Acad Sci USA* 95:3182–3187.
- Fuhs MC, Touretzky DS. 2006. A spin glass model of path integration in rat medial entorhinal cortex. *J Neurosci* 26:4266–4276.
- Fyhn M, Hafting T, Treves A, Moser EI, Moser MB. 2006. Coherence in ensembles of entorhinal grid cells. *Soc Neurosci Abstr* 68.9.
- Fyhn M, Hafting T, Treves A, Moser MB, Moser EI. 2007. Hippocampal remapping and grid realignment in entorhinal cortex. *Nature* 446:190–194.
- Giocomo LM, Zilli EA, Fransen E, Hasselmo ME. Temporal frequency of subthreshold oscillations scales with entorhinal grid cell field spacing. *Science* 315:1719–1722.
- Giovannini MG, Rakovska A, Benton RS, Pazzagli M, Bianchi L, Pepeu G. 2001. Effects of novelty and habituation on acetylcholine, GABA, and glutamate release from the frontal cortex and hippocampus of freely moving rats. *Neuroscience* 106:43–53.
- Gothard KM, Skaggs WE, McNaughton BL. 1996. Dynamics of mismatch correction in the hippocampal ensemble code for space: Interaction between path integration and environmental cues. *J Neurosci* 16:8027–8040.
- Gray JA, McNaughton N. 1983. Comparison between the behavioural effects of septal and hippocampal lesions: A review. *Neurosci Biobehav Rev* 7:119–188.
- Hafting T, Fyhn M, Molden S, Moser MB, Moser EI. 2005. Microstructure of a spatial map in the entorhinal cortex. *Nature* 436:801–806.
- Hafting T, Fyhn M, Moser MB, Moser EI. 2006. Phase precession and phase locking in entorhinal grid cells. *Soc Neurosci Abstr* 68.8.
- Hartley T, Burgess N, Lever C, Cacucci F, O'Keefe J. 2000. Modeling place fields in terms of the cortical inputs to the hippocampus. *Hippocampus* 10:369–379.
- Hasselmo ME. 2006. The role of acetylcholine in learning and memory. *Curr Opin Neurobiol* 16:710–715.
- Huxter J, Burgess N, O'Keefe J. 2003. Independent rate and temporal coding in hippocampal pyramidal cells. *Nature* 425:828–832.
- Jung MW, Wiener SI, McNaughton BL. 1994. Comparison of spatial firing characteristics of units in dorsal and ventral hippocampus of the rat. *J Neurosci* 14:7347–7356.
- Kamondi A, Acsady L, Wang XJ, Buzsaki G. 1998. Theta oscillations in somata and dendrites of hippocampal pyramidal cells in vivo: Activity-dependent phase-precession of action potentials. *Hippocampus* 8:244–261.
- Klink R, Alonso A. 1997a. Morphological characteristics of layer II projection neurons in the rat medial entorhinal cortex. *Hippocampus* 7:571–583.
- Klink R, Alonso A. 1997b. Muscarinic modulation of the oscillatory and repetitive firing properties of entorhinal cortex layer II neurons. *J Neurophysiol* 77:1813–1828.
- Kloosterman F, van Haeften T, Lopes da Silva FH. 2004. Two reentrant pathways in the hippocampal-entorhinal system. *Hippocampus* 14:1026–1039.
- Kramis R, Vanderwolf CH, Bland BH. 1975. Two types of hippocampal rhythmical slow activity in both the rabbit and the rat: Relations to behavior and effects of atropine, diethyl ether, urethane, and pentobarbital. *Exp Neurol* 49:58–85.
- Lengyel M, Szatmary Z, Erdi P. 2003. Dynamically detuned oscillations account for the coupled rate and temporal code of place cell firing. *Hippocampus* 13:700–714.
- Lever C, Wills T, Cacucci F, Burgess N, O'Keefe J. 2002. Long-term plasticity in hippocampal place-cell representation of environmental geometry. *Nature* 416:90–94.
- Maurer AP, Van Rhoads SR, Sutherland GR, Lipa P, McNaughton BL. 2005. Self-motion and the origin of differential spatial scaling along the septo-temporal axis of the hippocampus. *Hippocampus* 15:841–852.
- McNaughton BL, Barnes CA, O'Keefe J. 1983. The contributions of position, direction, and velocity to single unit activity in the hippocampus of freely-moving rats. *Exp Brain Res* 52:41–49.
- McNaughton BL, Battaglia FP, Jensen O, Moser EI, Moser MB. 2006. Path integration and the neural basis of the 'cognitive map'. *Nat Rev Neurosci* 7:663–678.
- Mitchell SJ, Ranck JB Jr. 1980. Generation of theta rhythm in medial entorhinal cortex of freely moving rats. *Brain Res* 189:49–66.
- Muller RU, Kubie JL. 1987. The effects of changes in the environment on the spatial firing of hippocampal complex-spike cells. *J Neurosci* 7:1951–1968.
- Muller RU, Kubie JL, Ranck JB Jr. 1987. Spatial firing patterns of hippocampal complex-spike cells in a fixed environment. *J Neurosci* 7:1935–1950.
- Muller RU, Bostock E, Taube JS, Kubie JL. 1994. On the directional firing properties of hippocampal place cells. *J Neurosci* 14:7235–7251.
- O'Keefe J. 1976. Place units in the hippocampus of the freely moving rat. *Exp Neurol* 51:78–109.
- O'Keefe J, Burgess N. 1996. Geometric determinants of the place fields of hippocampal neurons. *Nature* 381:425–428.
- O'Keefe J, Burgess N. 2005. Dual phase and rate coding in hippocampal place cells: Theoretical significance and relationship to entorhinal grid cells. *Hippocampus* 15:853–866.
- O'Keefe J, Dostrovsky J. 1971. The hippocampus as a spatial map. Preliminary evidence from unit activity in the freely-moving rat. *Brain Res* 34:171–175.

- O'Keefe J, Nadel L. 1978. *The Hippocampus as a Cognitive Map*. Oxford: Oxford University Press.
- O'Keefe J, Recce ML. 1993. Phase relationship between hippocampal place units and the EEG theta rhythm. *Hippocampus* 3:317–330.
- O'Keefe J, Burgess N, Donnett JG, Jeffery KJ, Maguire EA. 1998. Place cells, navigational accuracy, and the human hippocampus. *Philos Trans R Soc Lond B Biol Sci* 353:1333–1340.
- Petsche H, Stumpf C, Gogolak G. 1962. The significance of the rabbit's septum as a relay station between the midbrain and hippocampus. I. The control of hippocampus arousal activity by the septum cells. *Electroencephalogr Clin Neurophysiol* 14:202–211.
- Ranck JB Jr. 1984. Head-direction cells in the deep cell layers of the dorsal presubiculum in freely moving rats. *Soc Neurosci Abstr* 10:599.
- Redish AD, Touretzky DS. 1997. Cognitive maps beyond the hippocampus. *Hippocampus* 7:15–35.
- Sargolini F, Fyhn M, Hafting T, McNaughton BL, Witter MP, Moser MB, Moser EI. 2006. Conjunctive representation of position, direction, and velocity in entorhinal cortex. *Science* 312:758–762.
- Sharp PE. 1996. Multiple spatial/behavioral correlates for cells in the rat postsubiculum: Multiple regression analysis and comparison to other hippocampal areas. *Cereb Cortex* 6:238–259.
- Sharp PE. 1999. Subicular place cells expand or contract their spatial firing pattern to fit the size of the environment in an open field but not in the presence of barriers: Comparison with hippocampal place cells. *Behav Neurosci* 113:643–662.
- Skaggs WE, McNaughton BL, Wilson MA, Barnes CA. 1996. Theta phase precession in hippocampal neuronal populations and the compression of temporal sequences. *Hippocampus* 6:149–172.
- Somogyi P, Klausberger T. 2005. Defined types of cortical interneurone structure space and spike timing in the hippocampus. *J Physiol* 562:9–26.
- Stewart M, Fox SE. 1990. Do septal neurons pace the hippocampal theta rhythm? *Trends Neurosci* 13:163–168.
- Tahvildari B, Alonso A. 2005. Morphological and electrophysiological properties of lateral entorhinal cortex layers II and III principal neurons. *J Comp Neurol* 491:123–140.
- Taube JS, Muller RU, Ranck JB Jr. 1990. Head-direction cells recorded from the postsubiculum in freely moving rats. I. Description and quantitative analysis. *J Neurosci* 10:420–435.
- Thiel CM, Huston JP, Schwarting RK. 1998. Hippocampal acetylcholine and habituation learning. *Neuroscience* 85:1253–1262.
- Vanderwolf CH. 1969. Hippocampal electrical activity and voluntary movement in the rat. *Electroencephalogr Clin Neurophysiol* 26:407–418.
- Williams JM, Givens B. 2003. Stimulation-induced reset of hippocampal theta in the freely performing rat. *Hippocampus* 13:109–116.
- Winson J. 1976. Hippocampal theta rhythm. I. Depth profiles in the curarized rat. *Brain Res* 103:57–70.
- Witter MP, Moser EI. 2006. Spatial representation and the architecture of the entorhinal cortex. *Trends Neurosci* 29:671–678.